International Journal on Magnetic Particle Imaging
Vol 6, No 2, Suppl 1, Article ID 2009018, 3 Pages

Infinite Science Publishing

Proceedings Article

An upper bound for the frequency dependent energy of the 2-dimensional system function

C. Droigk[1,*] · M. Maass[1] · A. Mertins[1]

[1]Institute for Signal Processing, University of Lübeck, Lübeck, Germany
[*]Corresponding author, email: c.droigk@uni-luebeck.de

Abstract

In Magnetic Particle Imaging, the behavior of the system matrix energy in dependence of the frequency components has been investigated and relations have been observed. Due to the lack of a closed-form expression for the 2- or 3-dimensional system function, no expression for the energy has been obtained thus far. In this work, we use the recently found expression for the 2-dimensional system function to derive an upper bound for the energy of the 2-dimensional system function as a function of the frequency components. The comparison of the upper bound with the energy of a simulated system matrix confirms the results.

I Introduction

One common approach for reconstruction algorithms for Magnetic Particle Imaging (MPI) is the reconstruction using a system matrix in the temporal Fourier domain [1]. It has been observed that the energy of the system matrix varies in dependence of the frequency components in wave-like patterns [2]. With an expression of the 2-dimensional system function according to the Langevin model, we can obtain an upper bound for the system function energy. This might allow for more accurate signal-to-noise ratio (SNR) estimations and, thus, may result in better reconstruction quality.

I.I Expression for the 2D system function

The standard system matrix approach for reconstruction is to minimize

$$\|Sc-u\|_2^2+\lambda R(c) \tag{1}$$

with respect to c, where $S\in\mathbb{C}^{N\times M}$ is the system matrix in frequency space, $u\in\mathbb{C}^M$ contains the Fourier coefficients of the voltage measurement, and $c\in\mathbb{R}_+^N$ is the superparamagnetic iron oxide nanoparticle (SPIO) distribution. In [3] it has been shown that for the 2-dimensional case the spatio-temporal Fourier transform of the system function according to the Langevin model can be expressed as

$$\hat{\mathbf{s}}_k(\omega)=\frac{-i\omega_k}{|\det(\beta G)|}\mathcal{L}\left(\frac{G^{-1}\omega}{\beta}\right) \sum_{\lambda=-\infty}^{\infty}(-1)^\lambda J_{-k+\lambda N_B}\left(\omega_x\frac{A_x}{G_x}\right)J_{k-\lambda(N_B-1)}\left(\omega_y\frac{A_y}{G_y}\right). \tag{2}$$

The variables are $\omega_k=2\pi k/T_D$ with T_D the period length of the Lissajous trajectory, $\beta=\frac{\mu_0 m}{k_B T}$ with the vacuum permeability μ_0, the Boltzmann constant k_B, the temperature of the SPIOs T, the magnetic moment m, and $\mathcal{L}$ the Fourier transform of the 2D Langevin function. Furthermore, $G=\mathrm{diag}(G_x,G_y)$ and A_x,A_y are the applied gradients of the selection field and the amplitudes of the drive field, respectively, J_n is the Bessel function of first kind and n-th order, and N_B is a frequency divider for the 2D Lissajous trajectory, e.g. $T_D=\frac{N_B(N_B-1)}{f_B}$ with f_B the basis frequency of the MPI scanner.

With a similar approach as in [4], it can be shown that

Table 1: Parameters for the system matrix simulation.

Parameter	Value
Particle core diameter	30 nm
Temperature	293 K
Gradient strength $G_x = G_y$	$1\,\mathrm{T/m}/\mu_0$
Excitation amplitudes $A_x = A_y$	$0.0125\,\mathrm{T}/\mu_0$
Excitation frequencies f_x, f_y	$[2.5/96, 2.5/93]\cdot 10^6$ Hz

$$||J_n(x)x^\alpha||_{L^\infty} \leq C n^{\alpha-1/3} \tag{3}$$

with $\alpha \leq -n$, $n \in \mathbb{N}$ and a constant $C \in \mathbb{R}_+$. Using this formula, we derive an upper bound for the energy of the system function depending on the frequency components.

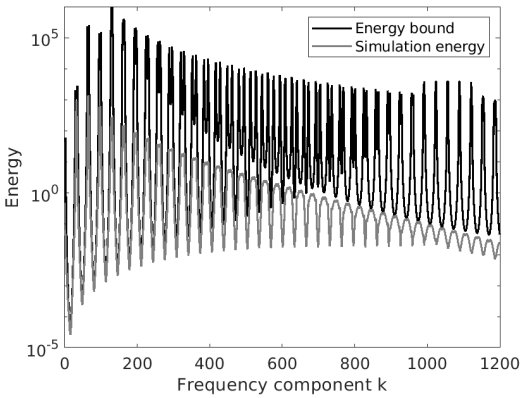

Figure 1: Comparison of derived upper bound for the energy of the system function and the energy of a simulated system matrix.

II Derivation

Let $\mathbf{A}(\omega)$ denote the prefactor of the sum in Eq. (2), i.e., $\mathbf{A}(\omega) = \frac{-i\omega_k}{|\det(\beta G)|}\mathcal{L}\left(\frac{G^{-1}\omega}{\beta}\right)$. With the triangle inequality and Hölder's theorem, we get for the energy of the system function

$$||\hat{\mathbf{s}}_k(\omega)||^2_{L^2} \leq \tag{4}$$
$$\left(\sum_{\lambda=-\infty}^{\infty} ||\frac{J_{k-\lambda N_B}\left(\omega_x \frac{A_x}{G_x}\right)}{\omega_x^2}\frac{J_{k-\lambda(N_B-1)}\left(\omega_y \frac{A_y}{G_y}\right)}{\omega_y^2}||_{L^\infty} ||\mathbf{A}(\omega)\omega_x^2\omega_y^2||_{L^2}\right).$$

With the help of eq. (3) we can show that

$$||\frac{J_{k-\lambda N_B}\left(\omega_x \frac{A_x}{G_x}\right)}{\omega_x^2}\frac{J_{k-\lambda(N_B-1)}\left(\omega_y \frac{A_y}{G_y}\right)}{\omega_y^2}||_{L^\infty} \leq C_1|k-\lambda N_B|^{-\frac{7}{3}}|k-\lambda(N_B-1)|^{-\frac{7}{3}} \tag{5}$$

holds. Note that the absolute orders of the Bessel functions must exceed 1, which means that the terms have no singularities. For the remaining norm in eq. (4) we get the result

$$||\mathbf{A}(\omega)\omega_x^2\omega_y^2||_{L^2} \leq C_2 k||e^{-|\alpha_1\omega_x|-|\alpha_2\omega_y|}\omega_x^2\omega_y^2||_{L^2} < \infty\,. \tag{6}$$

By inserting (5) and (6) into (4), we get

$$||\hat{\mathbf{s}}_k(\omega)||^2_{L^2} \leq \left(C_3 k \sum_{\lambda=-\infty}^{\infty} |(k-\lambda N_B)(k-\lambda(N_B-1))|^{-\frac{7}{3}}\right)^2 \tag{7}$$

for a $C_3 \in \mathbb{R}$. In fact, only one or two summands contribute significantly to the infinite sum. It can be shown that the indices of these summands are located inside the interval $\lfloor\frac{k}{N_B}\rfloor \leq \lambda \leq \lfloor\frac{k}{N_B-1}\rfloor$.

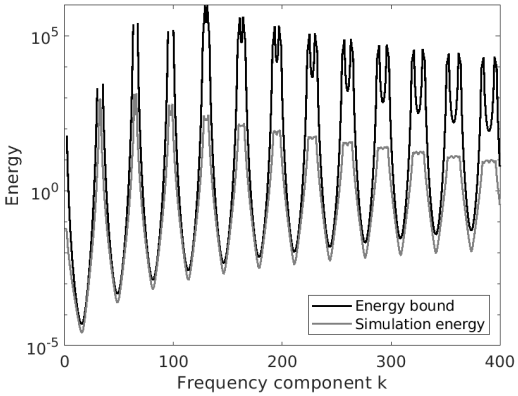

Figure 2: Detail look at the energy bound and the energy of the simulated system matrix.

III Numerical results

In this section we compare the derived upper bound with the energy of a simulated system matrix without any noise. The simulation was performed with the parameters given in Table 1. The energy with respect to the frequency components was computed and compared. The results are shown in Figs. 1 and 2. Since the constant C_3 in Eq. (7) is not known, the correct scaling of the upper bound cannot be derived accurately and is fitted manually. It can be seen that the energy bound has a similar decay for large frequency components k. Besides, the position of the local minima and maxima of the system matrix energy can be determined on the basis of the energy bound. With a proper scaling, the energy at the local minima is very close to the bound for frequency components up to about $k = 500$. This does not hold for larger k, but in this case the values at the local maxima are very close to the simulated results and decay in a similar manner.

10.18416/ijmpi.2020.2009018

IV Discussion

The results show that the derived bound has similar properties as the simulation and allows one to determine the frequency components with locally minimum and maximum energy. In spite of that, for $k > 700$ the bound has minima at the positions of the maxima and vice versa. This could be due to the use of Hölder's theorem in eq. (4). A direct estimation of the L_2-norm of the product of the Bessel functions with the term $\mathbf{A}(\omega)$ might better reflect the behavior of the simulation. It should also be noted that the estimation of the energy is identical for ω_x and ω_y. This means that the estimation is a bound for the energy of both receive coils.

V Conclusions

The behavior of the upper bound and the simulated energy show similar properties. Since it is quite exact for the low energy for components that are not too large, this information can be used for the estimation of the SNR and for the detection of frequency components with significant noise. For large frequency components the estimation of the local maxima might be used to determine a cut-off frequency.

Author's Statement

Research funding: The author state no funding involved.
Conflict of interest: Authors state no conflict of interest.

References

[1] J. Rahmer, J. Weizenecker, B. Gleich and J. Borgert, Signal encoding in magnetic particle imaging: properties of the system function, BMC Med Imaging, vol. 9(4), 2009.

[2] T. Knopp and T. M. Buzug, Magnetic particle imaging: an introduction to imaging principles and scanner instrumentation, Springer Science & Business Media, 2012.

[3] M. Maass and A. Mertins, On the Representation of Magnetic Particle Imaging in Fourier Space, Int. Journal on MPI, vol. 5(2), 2019.

[4] K. Stempak, A weighted uniform Lp-estimate of Bessel functions: a note on a paper of Guo, Proc. Am. Math. Soc., vol. 128(10), pp. 2943-2945, 2000.

10.18416/ijmpi.2020.2009018